

Localized contacts, stress concentrations and transient states in bent-lamination with viscoelastic adhesion. An analytical study

LAURA GALUPPI,
GIANNI ROYER-CARFAGNI¹

*Department of Industrial Engineering
University of Parma, Parco Area delle Scienze 181/A, I 43100 Parma, Italy
tel: +39-0521-905896, fax: +39-0521-905705
email: laura.galuppi@unipr.it, gianni.royer@unipr.it*

Abstract

An analytical study is presented for the bent-lamination of curved layered beams, a process consisting in gluing the constituent plies together after they have been elastically bent against a constraining negative mould. Possible applications range from *glued laminated timber* manufacturing, to *cold-lamination-bending* of structural glass. After removal of the constraint, the shear coupling through the glue maintains the curvature only partially, because the laminate suffers an initial spring-back followed by a long-term relaxation. The model problem considered here is that of two Euler-Bernoulli beams coupled by a thin viscoelastic adhesive layer. Within a variational approach, we analytically describe the relationship between the mould shape and the shape of the curved beam, which is time-dependent due to the viscosity of the adhesive layer. Localized contacts with the mould and stress concentrations may occur, depending upon the type of profile that is initially imposed. Comparison of the cases of *instantaneous* or *gradual* release of the contact with the mould, evidences a remarkable reduction of the transient state of stress in the second case.

¹Corresponding author.

Keywords: Bent-lamination; A. Laminate; B. Interface; C. Modelling; C. Stress concentrations

Contents

| | | |
|----------|---|-----------|
| 1 | Introduction | 3 |
| 2 | The model problem | 5 |
| 2.1 | The bent-lamination process | 5 |
| 2.2 | Strain energy and governing equations | 7 |
| 2.3 | Approach <i>à la</i> Newmark | 8 |
| 3 | Bent-lamination and instantaneous release | 10 |
| 3.1 | Springing back and relaxation in Phase <i>II</i> | 10 |
| 3.2 | Transient states | 11 |
| 3.3 | Stress concentrations in the adhesive layer | 13 |
| 3.4 | How to avoid stress concentrations in the adhesive interface | 14 |
| 4 | Bent-lamination and gradual release | 16 |
| 4.1 | Stage <i>A</i> : distributed contact | 17 |
| 4.1.1 | Limit cases of null adhesion or stiff adhesion | 17 |
| 4.1.2 | Compliant adhesive layer | 18 |
| 4.1.3 | Results and comparisons. | 20 |
| 4.2 | Stage <i>B</i> : pointwise contact | 23 |
| 4.2.1 | Compliant adhesive layer | 23 |
| 4.2.2 | Results and comparisons. | 23 |
| 4.3 | Comparison between instantaneous and gradual release in case of viscoelastic adhesion | 25 |
| 5 | Conclusions | 27 |

1. Introduction

In recent years, layered structures made by the composition of elastic layers bonded by adhesive interlayers have been increasingly used in many applications, in civil as well as aerospace, aeronautical, automobile and naval constructions. An interesting technique to obtain low-cost curved elements is bent-lamination, which consists in gluing the constituent plies together after they have been elastically bent against a constraining curved mould. Releasing the package, the curvature is at least partially maintained through the shear coupling of the plies *via* the adhesive layers.

An example of bent lamination products is “*Glulam*” (*Glued laminated timber*), composed of suitably prepared wood sheets glued together with moisture-resistant adhesives [1]. Arches are glued and cured in curved forms, by constraining the package to the negative mould with physical clamps or a vacuum press that define their shape. Once the adhesive is dry, the resulting part will substantially hold its shape, even if the element may suffer an initial spring-back followed by a slow relaxation due to the viscoelastic properties of the adhesive layers [2]. Another example is laminated glass. Widely used in architecture thanks to its sound-insulation capability and fail-safe post-glass-breakage response, it is composed by two (or more) glass plies bonded together by a polymeric viscoelastic interlayer [3, 4]. A promising technique to obtain low-cost curved glazing consists in cold-bending the not-yet-coupled glass-interlayer assembly in the desired shape and, in this constrained state, performing the lamination process in an autoclave [5, 6, 7]. After that adhesion takes place, it is the bond of the glass through the interlayer that maintains the curvature when the constraints are removed, even if the temperature-dependent viscoelastic properties of the interlayer [8, 9, 10, 11] may lead to a slow change of the configuration [7].

In all cases, the rheologic effects must be precisely predicted to obtain the prescribed curved surface. The model problem that is considered here is that of two external layers with axial and bending stiffness glued by a thin viscoelastic adhesive interlayer, which can only provide the shear coupling of the external layers. In other words, the role of the interlayer is to provide shear stresses that contribute to the gross bending stiffness of the composite package, keeping unchanged the relative distance between the external layers [12, 13, 14]. The laminated beam is assembled by bonding the external plies through the interlayer after having been curved against a constraining mould. Assuming that the response of the adhesive is viscoelastic, the problem is to calculate the time-dependent variation of the beam shape, as well as the redistribution of stress in the components.

In the analytical model, the external plies are Euler-Bernoulli beams and the adhesive is a viscoelastic layer which has negligible longitudinal stiffness with respect to the beams, presents negligible strain in transversal direction so to suppose invariant its thickness, and has variable stiffness in shear. More precisely, the viscoelasticity is considered by modeling the interlayer as a linear elastic body, characterized by a proper temperature- and time-dependent shear modulus. This approximation, usually referred to as the *quasi-elastic* method, is equivalent to neglecting the memory effect of viscoelasticity [10].

In Section 2, a variational approach to this problem, based on the minimization of the total strain energy functional, is used to determine the governing differential equations and

boundary conditions under the hypothesis that the curvature is moderate². The problem is solved by developing a method originally proposed by Newmark *et al.* [15] to study the elastic coupling through shear studs of steel-concrete composite bridge decks. Such a formulation allows to write the governing equilibrium equations as a function of the vertical displacement only, for those cases in which the overall bending moment in the beam is statically determined. Appropriate boundary conditions either on the vertical displacement field and on the shear stress transmitted by the interlayer need to be added. The so-obtained governing equation allows to evaluate the relationship between the prescribed deformed shape in the forcing phase, i.e., the mould shape, and the beam relaxation, as well as the contact reactions and the resulting state of stress in the constituent layers.

The case of *instantaneous* removal of the constraining mould is investigated, with particular reference to the effect of the mould shape on both the constraint reactions and the transient state of stress field consequent to the relaxation of the adhesive layer. In Section 3, it will be analytically proved that the most common case of constant-curvature mould leads to shear stress concentrations at the beam ends. The higher the shear stiffness of the adhesive layer, the more critical is its state of stress and, in the limit case of infinite-stiff adhesive, the shear stress becomes singular because concentrated forces at the extremities are necessary to guarantee equilibrium. This phenomenon presents analogies with the findings of the keystone contributions by Puppo and Evensen [16] and Pipes and Pagano [17], that, in the seventies, investigated the interlaminar shear stress in composite laminates. Remarkably, it will be shown that if the mould profile is sinusoidal, the stress peaks are smoothen out even when the shear modulus of the adhesive is high. When the bending curvature is moderate, the difference between the sinusoidal and the constant curvature shapes is inappreciable, so that the aesthetics appearance is not affected.

Noteworthy advantages in terms of stress state can be obtained not only through the optimization of the the mould profile, but also by designing a gradual release of the laminated beam. In Section 4, we study the contact problem by assuming that time-decreasing external loads press the beam on the mould and produce a progressive decrease of the contact area, until the laminate is completely released. It will be shown that, whereas in the limit cases of free-sliding plies (null shear modulus of the adhesive layer) or rigidly bonded plies (infinite shear stiffness of the adhesive) the constant-curvature mould exerts concentrated reaction forces at the borders of the contact zone, in the intermediate case of elastic connection also a distributed pressure comes into play in the contact area. The nature and type of contact depends upon the time-dependent shear stiffness of the interlayer and the unloading history. By properly designing the release phase it is possible to bypass the most severe stress states that occur in the case of instantaneous unloading, thus reducing the risks of delamination.

²This hypothesis is met both for the cold-lamination bending of glass, where the radius of curvature is of the order of several meters while glass thickness is just a few millimeters, and for Glulam, for which the radius of curvature is generally limited to be between 100 and 125 times the thickness of the laminate.

2. The model problem

The problem that will be considered is indicated in Figure 1a. Two external Euler-Bernoulli beams, of length L , width b , Young's modulus E and thickness h_1 and h_2 , respectively, are coupled by an adhesive layer of thickness h . Such layer is supposed so thin that its axial and bending stiffness are negligible, but it can provide the shear coupling of the beams through its shear modulus $G(t)$, supposed time-dependent.

Introduce a right-handed orthogonal reference frame (x, y) , with x parallel to the beam axis and y directed upwards, so that $-L/2 \leq x \leq L/2$ denotes the reference configuration of the body, and define the geometrical parameters

$$A_i = h_i b, I_i = \frac{bh_i^3}{12} \quad (i = 1, 2), \quad H = h + \frac{h_1 + h_2}{2}, \quad A^* = \frac{A_1 A_2}{A_1 + A_2}, \quad I_{tot} = I_1 + I_2 + A^* H^2, \quad (2.1)$$

where I_{tot} represents the moment of inertia of the cross sections of the beams properly spaced of the adhesive interlayer gap. Under the hypothesis that strains are small and rotations moderate, the kinematics is completely described by the vertical displacement $v(x, t)$, the same for the two glass components, and the horizontal displacements $u_1(x, t)$ and $u_2(x, t)$ of the centroid of the upper and lower beams, respectively (Figure 1b). The shear strain in the interlayer consequently reads [4]

$$\gamma(x, t) = \frac{u_1(x, t) - u_2(x, t) + v(x, t)' H}{h}, \quad (2.2)$$

where, here and further, $'$ denotes differentiation with respect to x .

Following the *quasi-elastic* approximation [10], the adhesive is modeled as a linear elastic material, characterized by a proper time-dependent secant shear modulus to take into account viscoelastic effects, so that the shear stress $\tau(x, t)$ is given by

$$\tau(x, t) = G(t)\gamma(x, t). \quad (2.3)$$

One may assume that the viscoelasticity of the adhesive layer follows a Maxwell-Wiechert model, so that its shear modulus decays with time according to a Prony series [18].

At least as a first order approximation, the beam curvature will be considerate moderate, an hypothesis that is certainly met in most cases of practical importance [5, 19, 2].

2.1. The bent-lamination process

The composite beam is supposed to undergo a process consisting in two different phases.

- *Phase I, distortion.* The not-yet-bonded package, composed by the beams and the adhesive layer, is constrained to bend in the desired shape (Figure 2a). A relative displacement occurs between the faces of the beams in contact with the adhesive layer, which will be considered in the following as a *distributed shear dislocation* [7].

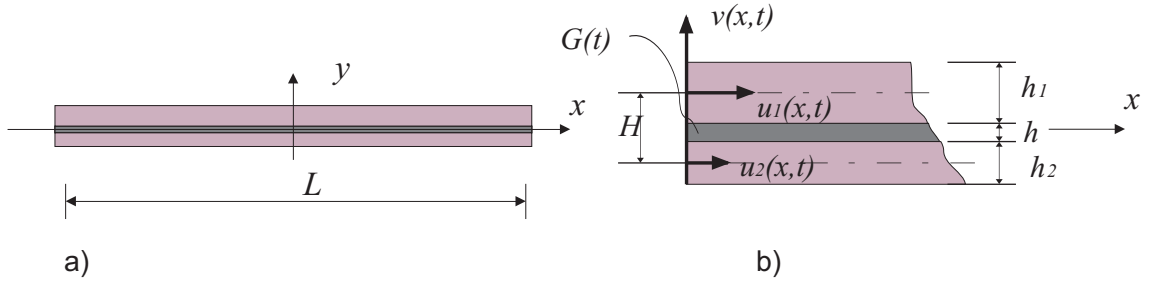


Figure 1: Sandwich beam with viscoelastic shear-compliant core: a) longitudinal view and b) magnification, with relevant displacement components.

- *Phase II, transient.* After the adhesion is complete, the constraints are removed. Now, it is the shear coupling provided by the adhesive layer that maintains the curvature. However, as a consequence of the viscoelasticity of the adhesive layer, the curved laminate exhibits an initial spring-back, followed by a long-term relaxation due to the decay of the shear-coupling of the beams. As a consequence, the actual curvature is different from the curvature of the mould (Figure 2b).

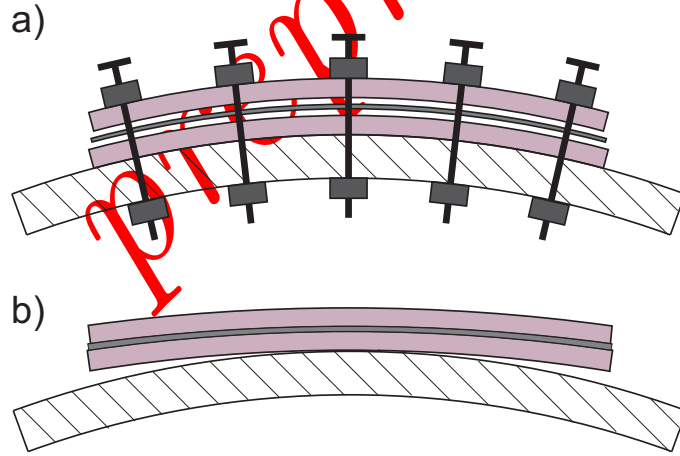


Figure 2: Cold-lamination-bending process. a) Phase *I*: cold bending of the uncoupled package onto the negative mould; b) phase *II*: springback and relaxation after release.

Assume that the bending moment $M(x, t)$ acting in the whole composite beam is positive when $v''(x, t) > 0$, while constraint reaction forces per unit length $q(x, t) = -M''(x, t)$ are positive when directed downward. Here and further, parameters and functions referring to the two aforementioned phases will be labelled with the subscript *I* and *II*, respectively.

During phase *I*, the inertia of the not-yet-bonded package is simply given by $I_1 + I_2$. If the profile of the mould is described by the function $\bar{v}(x)$, then $v_I(x, t) = \bar{v}(x)$. The bending moment and the constraint reactions are constant in time and read

$$M_I(x) = E(I_1 + I_2) \bar{v}''(x), \quad q_I(x) = -M_I''(x) = -E(I_1 + I_2) \bar{v}''''(x). \quad (2.4)$$

Moreover, since the layers are uncoupled, the shear stress in the adhesive layer, as well as the axial forces in the two beams, are null. Setting $u_1(x, t) = u_2(x, t)$ in (2.2), the shear dislocation of the two beams in phase I , associated with null shear stress, is given by [7]

$$\gamma_I(x, t) = \bar{\gamma}(x) = \frac{H}{h} \bar{v}'(x), \quad \tau_I(x, t) = 0. \quad (2.5)$$

In phase II the shear stress transmitted by the adhesive layer is proportional to the shear strain associated with springing back and relaxation, i.e., to the difference between the actual shear strain and the initial distortion $\bar{\gamma}(x)$. From (2.2) and (2.3), one has

$$\gamma_{II}(x, t) = \frac{u_{1;II}(x, t) - u_{2;II}(x, t) + v'_{II}(x, t)H}{h}, \quad \tau_{II}(x, t) = G(t)[\gamma_{II}(x, t) - \bar{\gamma}(x)]. \quad (2.6)$$

More details for this *distributed dislocation approach* can be found in [7].

2.2. Strain energy and governing equations

During phase II , the strain energy of the beam $-L/2 \leq x \leq L/2$ at the time t can be written in the form [20]

$$\begin{aligned} \mathfrak{E}[u_{1;II}(x, t), u_{2;II}(x, t), v_{II}(x, t)] = & \\ & \int_{-L/2}^{L/2} \left\{ \frac{1}{2} \left[E(I_1 + I_2) [\bar{\gamma}'_{II}(x, t)]^2 + EA_1 [u'_{1;II}(x, t)]^2 + EA_2 [u'_{2;II}(x, t)]^2 \right. \right. \\ & + \frac{Gb}{h} [u_{1;II}(x, t) - u_{2;II}(x, t) + v'_{II}(x, t)H]^2 - Gb [u_{1;II}(x, t) - u_{2;II}(x, t) + v'_{II}(x, t)H] \bar{\gamma}(x) \\ & \left. \left. + q(x, t) v_{II}(x, t) \right\} dx, \end{aligned} \quad (2.7)$$

where $q(x, t)$ represents the constrain reactions.

For fixed t , the first variation of the functional with respect to the variations $u_{1;II}(x, t) + \delta u_{1;II}(x, t)$, $u_{2;II}(x, t) + \delta u_{2;II}(x, t)$ and $v_{II}(x, t) + \delta v_{II}(x, t)$ gives, respectively, the following Eulers equilibrium equations

$$\begin{aligned} E(I_1 + I_2)v_{II}''''(x, t) - GbH[\gamma'_{II}(x, t) - \bar{\gamma}'(x)] + q(x, t) &= 0, \\ EA_1 u_1''(x, t) &= Gb[\gamma_{II}(x, t) - \bar{\gamma}(x)], \\ EA_2 u_2''(x, t) &= -Gb[\gamma_{II}(x, t) - \bar{\gamma}(x)], \end{aligned} \quad (2.8)$$

with gemoetric/natural boundary conditions of the form

$$\begin{aligned}
& \left[-E(I_1 + I_2)v_{II}'''(x, t) + GbH(\gamma_{II}(x, t) - \bar{\gamma}(x))\delta v_{II}(x, t) \right]_{-L/2}^{L/2} = 0, \\
& \left[E(I_1 + I_2)v_{II}''(x, t)\delta v_{II}'(x, t) \right]_{-L/2}^{L/2} = 0, \\
& \left[EA_1u'_{1;II}(x, t)\delta u_{1;II}(x, t) \right]_{-L/2}^{L/2} = 0, \\
& \left[EA_2u'_{2;II}(x, t)\delta u_{2;II}(x, t) \right]_{-L/2}^{L/2} = 0.
\end{aligned} \tag{2.9}$$

Condition (2.8)₁ is the equilibrium in the y -direction of a beam with inertia $I_1 + I_2$ under the external load $q(x, t)$ and under a distributed moment per unit length $\tilde{m}(x, t) = -bH\tau_{II}(x, t)$, which accounts for the stiffening contribution of the shear coupling through the adhesive [4]. Moreover, in (2.9)₁ the quantity

$$V^*(x, t) = -E(I_1 + I_2)v_{II}'''(x, t) + GbH[\gamma_{II}(x, t) - \bar{\gamma}(x)] = -E(I_1 + I_2)v_{II}'''(x, t) + bH\tau_{II}(x, t), \tag{2.10}$$

can be regarded as a fictitious shear force, accounting for the effects of the distributed moment per unit length.

By defining the axial forces $N_{i;II}(x, t) = EA_i u'_{i;II}(x, t)$, $i = 1, 2$, the equilibrium equations (2.8) may be rewritten as

$$\begin{aligned}
& E(I_1 + I_2)v_{II}'''(x, t) + \tilde{m}'(x, t) + q(x, t) = 0, \\
& N'_{1;II}(x, t) = b\tau_{II}(x, t), \\
& N'_{2;II}(x, t) = -b\tau_{II}(x, t),
\end{aligned} \tag{2.11}$$

whose interpretation in terms of equilibrium is immediate.

2.3. Approach à la Newmark

It is useful to re-arrange the governing equations following an argument proposed by Newmark [15], which allows to write (2.8)₁ as a function of the vertical displacement $v_{II}(x, t)$ only when the bending moment in the laminated beam is known, i.e., whenever the structure is statically determined.

The bending moment $M_{II}(x, t)$ acting in phase II is due to the sum of the bending moments in the two beams, i.e., $M_{1;II}(x, t) = EI_1 v_{II}''(x, t)$ and $M_{2;II}(x, t) = EI_2 v_{II}''(x, t)$, and the contribution of the axial forces $N_{1;II}(x, t)$ and $N_{2;II}(x, t)$ multiplied by the level arm H . Combining the second and third of (2.11), one can demonstrate [4, 20] that $N_{1;II}(x, t) = -N_{2;II}(x, t)$ and, hence,

$$M_{II}(x, t) = E(I_1 + I_2)v_{II}''(x, t) - N_{1;II}(x, t)H = E(I_1 + I_2)v_{II}''(x, t) + N_{2;II}(x, t)H. \tag{2.12}$$

It is also possible to find the expressions for the axial displacement fields as function of the vertical displacement and of the external bending moment (see [10] and [20] for the details).

These, together with equation (2.3) and (2.6)₂, lead to the relationship

$$\tau'_{II}(x, t) = \frac{G(t)}{hA^*H} \left[I_{tot} v''_{II}(x, t) - \frac{M_{II}(x, t)}{E} \right] - G(t) \bar{\gamma}'(x). \quad (2.13)$$

By substituting (2.13) in (2.8)₁ and by recalling that $q_{II}(x, t) = -M''_{II}(x, t)$, the first equilibrium equation can be written in the form

$$E(I_1 + I_2)v''''_{II}(x, t) - \frac{bI_{tot}G(t)}{hA^*} v''_{II}(x, t) - G(t)Hb \bar{\gamma}'(x) + \frac{bG(t)}{hEA^*} M_{II}(x, t) - M''_{II}(x, t) = 0. \quad (2.14)$$

Two important limit cases are those of free-sliding beams (null stiffness of the adhesive layer), or rigidly bonded beams (infinite shear stiffness of the adhesive), which, borrowing terms from the literature on laminated glass, will be referred to as the *layered* and *monolithic* limits. In the sequel, quantities referred to these limits will be denoted by the subscript L and M , respectively. In such borderline cases, (2.14) becomes

$$\begin{aligned} E(I_1 + I_2)v''''_{II;L}(x, t) - M''_{II}(x, t) &= 0, \\ -EI_{tot} v''_{II;M}(x, t) - EHbA^* \bar{\gamma}'(x) + M_{II}(x, t) &= 0. \end{aligned} \quad (2.15)$$

If the external constraint is *instantaneously* removed after that adhesion has taken place (phase *II*), $M_{II}(x, t) = 0$ and (2.14) can be simplified in the form

$$E(I_1 + I_2)v''''_{II}(x, t) - \frac{bI_{tot}G(t)}{hA^*} v''_{II}(x, t) - G(t)Hb \bar{\gamma}'(x) = 0. \quad (2.16)$$

Observed that $G(t)Hb \bar{\gamma}'(x)$ plays the role of an additional load acting on the beam that tends to keep it in the deformed configuration. Since, in general, the shear modulus of the interlayer $G(t)$ decreases with time, this is a time-decreasing contribution.

Once the vertical displacement is known from (2.14), the shear stress in the interlayer comes from equation (2.13) and, by recalling equation (2.12), the maximum normal stress σ_i in the i -th beam, $i = 1, 2$, can be evaluated through expressions of the type [21]

$$\begin{aligned} |\sigma_{i;II}(x, t)| &= \left| \frac{N_{i;II}(x, t)}{A_i} \pm \frac{M_{i;II}(x, t)}{I_i} \frac{h_i}{2} \right| \\ &= \left| \frac{M_{II}(x, t) - E(I_1 + I_2)v''_{II}(x, t)}{HA_i} \pm E \frac{h_i}{2} v''_{II}(x, t) \right|. \end{aligned} \quad (2.17)$$

The order of the relevant differential equations confirm the obvious conclusion that in the case of symmetric bending (symmetric vertical displacement), the distribution of shear stress is antisymmetric.

3. Bent-lamination and instantaneous release

In the following, reference will be made to the case of a constant-curvature constraint, which represents the most common condition in the practice. Under the hypotheses of small deflection, the shape of the mould is approximated by the parabola

$$\bar{v}(x) = \frac{K}{2} \left(x^2 - \frac{L^2}{4} \right), \quad M_I(x) = E(I_1 + I_2)K = \text{const}, \quad (3.1)$$

where K is representative of the curvature. The corresponding distributed shear dislocation, given by (2.6), is consequently $\bar{\gamma}(x) = \frac{HK}{h}x$.

It will be assumed, in the following, that in phase I a perfect contact is obtained between the laminated package and the mould. However, it should be mentioned that, if the contact is produced by two external forces P_I applied at the beam ends, as shown in Figure 3a, the constraint reactions would be represented by concentrated forces of Figure 3b. In fact ([22], Chapt. 5), since the bending moment is constant in the contact region $x \in [-d_I, d_I]$, no distributed constrain reactions are present because $q_I(x) = -M_I''(x) = 0$. The relation between the applied load P_I and the distance d_I may be evaluated by requiring the continuity of the bending moment³ at $x = \pm d_I$, so that

$$-P_I(L/2 - d) - M_I = E(I_1 + I_2)K. \quad (3.2)$$

However, the Euler Bernoulli beam theory clearly fails when $L/2 - d_I$ becomes of the same order of the beam thickness.

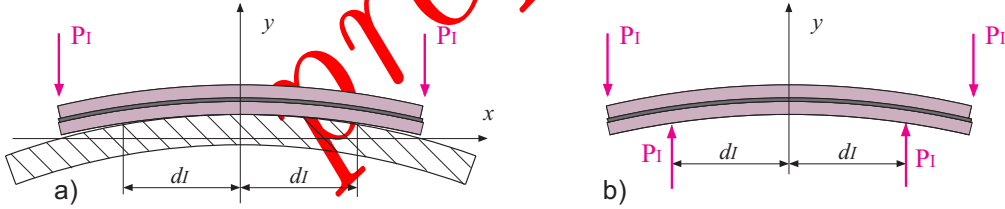


Figure 3: Constant-curvature distortion in phase I ; a) action of concentrated forces at the beam's ends and b) constraint reactions from the mould.

3.1. Springing back and relaxation in Phase II

In the case of instantaneous release of the beam after adhesion, the vertical displacement during Phase II may be evaluated by solving equation (2.16), together with boundary conditions $v''_{II}(\pm L/2, t) = 0$, $v_{II}(0, t) = \bar{v}(0) = -KL^2/8$ and $v'_{II}(0, t) = 0$, $\forall t$. The result is

³The continuity of the bending moment is implicit because the mould cannot react with a concentrated moment if the contact constraint is supposed to be, as in the case at hand, unilateral.

$$v_{II}(x, t) = \frac{KH^2A^*}{\alpha^2(t)I_{tot}} \left[-\frac{1 - \cosh(\alpha(t)x)}{\cosh(\alpha(t)L/2)} + \frac{\alpha^2(t)x^2}{2} \right] - \frac{KL^2}{8}, \quad \alpha(t) = \sqrt{\frac{bI_{tot}G(t)}{hA^*E(I_1 + I_2)}}. \quad (3.3)$$

The initial spring-back may be evaluated by posing $\alpha(t) = \alpha(0)$ in (3.3).

The expression (3.3) allows to recover the response of the layered beam in the two borderline cases of layered and monolithic limit. In the case of frictionless sliding of the beam (layered limit), $G(t) = 0 \Rightarrow \alpha(t) \rightarrow 0$, and one finds

$$v_{II;L}(x) = \lim_{\alpha(t) \rightarrow 0} v_{II}(x, t) = -\frac{KL^2}{8}. \quad (3.4)$$

In words, since the interlayer offers no shear coupling, the beam returns back to its initial undeformed configuration. In the monolithic limit when $G(t) \rightarrow \infty \Rightarrow \alpha(t) \rightarrow \infty$, one has

$$v_{II;M}(x) = \lim_{\alpha(t) \rightarrow +\infty} v_{II}(x, t) = \frac{K}{2} \left[\frac{A^*H^2}{I_{tot}} x^2 - \frac{L^2}{4} \right] = \bar{v}(x) - \frac{K}{2} \frac{I_1 + I_2}{I_{tot}} x^2, \quad (3.5)$$

$$v''_{II;M} = K \left[1 - \frac{I_1 + I_2}{I_{tot}} \right] = \frac{M_I}{E(I_1 + I_2)} = \frac{M_I}{EI_{tot}}.$$

This means that, when the adhesive layer is shear-rigid, the springing-back curvature is proportional to the inertia I_{tot} of the monolith.

For the sake of illustration, consider the case $h_1 = h_2 = 20$ mm, $E = 12000$ MPa, $h = 0.5$ mm, $L = 150 \cdot h_1$ and $b = 50 \cdot h_1$, forced on a mould of radius $1/K = 300 \cdot h_1$. Figure 4 shows the vertical displacement $v_{II}(x, t)$ as a function of $x \in [-L/2, L/2]$ for various values of t , and consequently of $G(t)$.

3.2. Transient states

The shear stress in the adhesive layer can be evaluated by posing $M_{II}(x, t) = 0$ in (2.13). Since by symmetry and equilibrium $\int_{-L/2}^{L/2} \tau_{II}(x, t) dx = 0, \forall t$, one finds

$$\tau_{II}(x, t) = -\frac{G(t)HK}{h\alpha(t)} \frac{\sinh(\alpha(t)x)}{\cosh(\alpha(t)L/2)} = -\alpha(t)HKA^*E \frac{I_1 + I_2}{bI_{tot}} \frac{\sinh(\alpha(t)x)}{\cosh(\alpha(t)L/2)}. \quad (3.6)$$

Observe that for high values of $\alpha(t)$ the shear stress tends to concentrate in the neighborhood of the beam's ends. The higher the shear modulus of the adhesive, the most severe is the corresponding state of stress. The maximum axial stress acting on the i -th beam can be evaluated through (2.17) with $M_{II}(x, t) = 0$ and reads

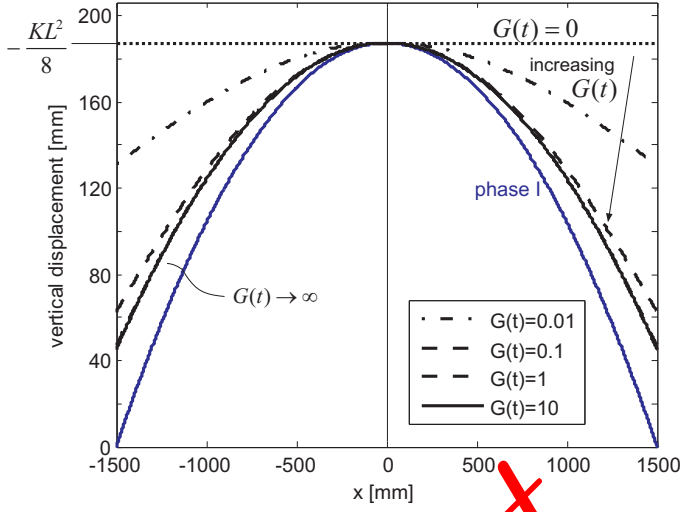


Figure 4: Constant-curvature bent-lamination. Vertical displacement in Phase II for various values of $G(t)$.

$$|\sigma_{i,II}(x,t)| = E \left| \left(\frac{-(I_1 + I_2)}{HA_i} \pm \frac{h_i}{2} \right) v''_{II}(x) \right| \quad (3.7)$$

$$= \frac{EKH^2 A'}{I_{tot}} \left(\frac{I_1 + I_2}{HA_i} + \frac{h_i}{2} \right) \left[1 - \frac{\cosh(\alpha(t)x)}{\cosh(\alpha(t)L/2)} \right]. \quad (3.8)$$

For the same example proposed at the end of Section 3.1, Figures 5a and 5b show, as a function of x , the shear stress in the adhesive layer and the maximum axial stress in the beams $\sigma_{max}(t)$ (in absolute value), respectively.

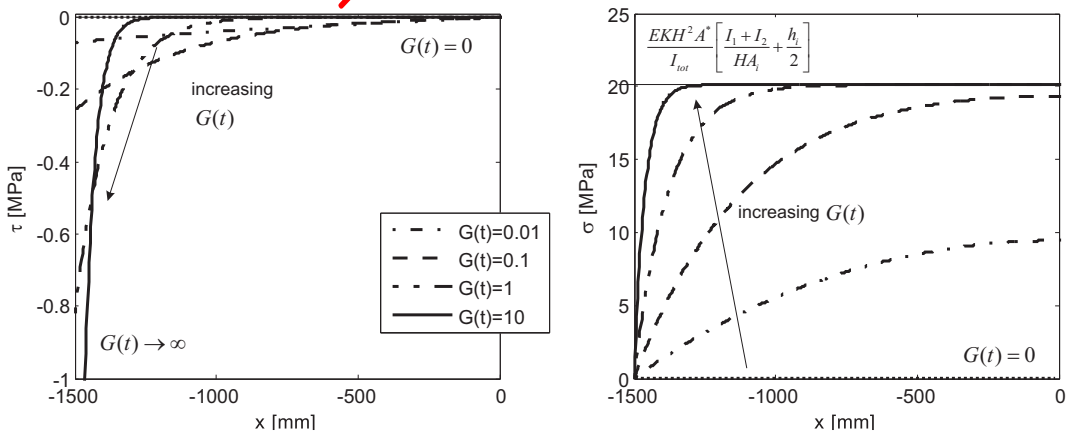


Figure 5: Constant-curvature bent-lamination. Shear stress in the adhesive layer and maximum axial stress in the beams for various values of $G(t)$.

Obviously, when $G(t) \rightarrow 0$ the stresses are null. When instead $G(t) \rightarrow \infty$, it can be analytically verified that the axial stress tends to a constant, whereas the shear stress localizes at $x = \pm L/2$, that is

$$\lim_{G(t) \rightarrow \infty} \sigma_{i;II}(x, t) = \lim_{\alpha(t) \rightarrow \infty} \sigma_{i;II}(x) = \frac{EKH^2A^*}{I_{tot}} \left[\frac{I_1 + I_2}{HA_i} + \frac{h_i}{2} \right], \quad (3.9)$$

$$\lim_{G(t) \rightarrow \infty} \tau_{II}(x, t) = \lim_{\alpha(t) \rightarrow \infty} \tau_{II}(x, t) = \begin{cases} -\infty & x = -L/2, \\ 0 & |x| < L/2, \\ +\infty & x = L/2. \end{cases}$$

In other words, the adhesive layers needs to transmit concentrated shear forces F at the beam's ends. The magnitude of F acting at $x = -L/2$ can be evaluated as

$$F = \lim_{\alpha(t) \rightarrow \infty} b \int_{-L/2}^0 \tau_{II}(x, t) dx = \lim_{\alpha(t) \rightarrow \infty} EA^*HK \frac{I_1 + I_2}{I_{tot}} \frac{\cosh(\alpha(t)L/2) - 2}{\cosh(\alpha(t)L/2)} = -EA^*HK \frac{I_1 + I_2}{I_{tot}}. \quad (3.10)$$

In the next Section, this finding will be discussed more in detail.

3.3. Stress concentrations in the adhesive layer

In phase II , when $G(t) \rightarrow \infty$ the external bending moment is null and the beam curvature, given by (3.5), is constant. Hence, from (2.12), one has

$$M_{II}(x) = E(I_1 + I_2)v''_{II}(x) - N_{1,II}(x)H = E(I_1 + I_2)v''_{II}(x) + N_{2,II}(x)H = 0. \quad (3.11)$$

which gives that $N_{1,II}(x) = -N_{2,II}(x) = \text{const}$. But the equilibrium equations (2.8)₂₋₃ in horizontal direction imply that

$$N_{1,II} = -N_{2,II} = \int_0^x \tau_{II}(\xi) d\xi = \text{const}. \quad (3.12)$$

Such a requirement, together with boundary conditions (2.9)₂ and (2.9)₃ ($N_{i,II}(\pm L/2) = 0$), would imply a null distribution of the shear stress along the beam (Figure 6a), and the paradoxical conclusion that the adhesive is inactive. It is then necessary to assume the occurrence of concentrated shear forces F in correspondence of the beam's ends (Figure 6b), as predicted by the limit (3.9). From equilibrium one finds

$$N_1(x) = -N_2(x) = F, \quad \Rightarrow F = -\frac{M(x) - E(I_1 + I_2)v''_{II}(x)}{H} = -EA^*HK \frac{I_1 + I_2}{I_{tot}}, \quad (3.13)$$

which coincides with the conclusion of (3.10).

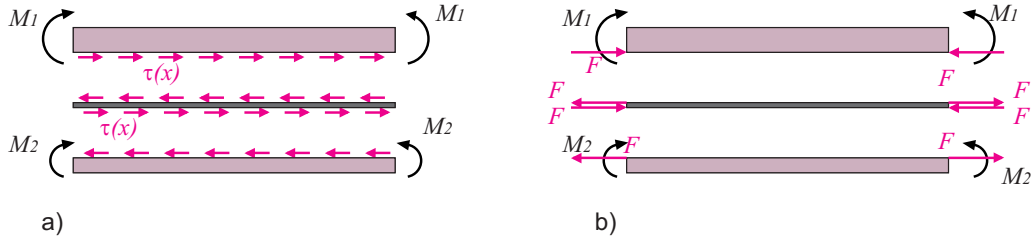


Figure 6: Shear stress transmitted by the adhesive layer. a) Continuous shear stress distribution and b) singular stress distribution.

The phenomenon of stress intensification in laminates has been the subject of a very large number of studies. Already in the seventies Puppo and Evensen [16] investigated the interlaminar shear stress in composite laminates under generalized plane stress, modeled as two anisotropic layers separated by an isotropic inner layer able to transmit shear stress only. The problem of a finite symmetrical laminate under uniform unidirectional deformation was analytically solved, and the distribution of the shear stress in the inner layer was found to be of the same type of (3.6), that is, hyperbolic sinusoidal with maximum shear stress at the plate borders. In their seminal work [17], Pipes and Pagano considered the response of a finite-width composite laminate under uniform axial strain, treated within classical elasticity theory and solved by means of finite differences analysis. Supposing that the interface thickness was negligible and the bonding between the plies was perfect (continuity of the displacement fields across the interface), the interlaminar shear stress appeared to grow unboundedly in the neighborhood of the plate free edges. Similar phenomena have been observed by Salamon [23], reporting the results of a numerical finite-difference investigation of the interlaminar stresses induced in a layered laminate subject to pure bending. Several works, also in recent years, are focused on the singularities in interlaminar stress due to thermal effects in composites (see, among the others, [24, 25, 26, 27]). Generally speaking, the interlaminar stresses which develop in the boundary regions along the free edges of a composite laminates are identified as causes of edge delamination phenomena. This relationship has been investigated, even in recent years, both from the analytical [28, 29, 30] and the experimental [31, 32] point of view.

There may be various countermeasures to avoid, or at least mitigate, the stress concentrations in the adhesive layers. One possibility, discussed in the next section, consists in slightly changing the shape of the constraining mould. However, as it will be discussed in Section 4, also a *gradual* release from the constraints during Phase *II* may contribute to smoothen out the localization of stress at the adhesive interface.

3.4. How to avoid stress concentrations in the adhesive interface

Consider a (co)sinusoidal shape for the constraining mould and the consequent bending moment in Phase *I* of the type

$$\bar{v}(x) = v_{max} \cos\left(\frac{\pi x}{L}\right), \quad M_I(x) = -E(I_1 + I_2) \frac{\pi^2}{L^2} \cos\left(\frac{\pi x}{L}\right); \quad (3.14)$$

where v_{max} denotes the initial camber. The constraint reaction is $q_I(x) = -M_I''(x) = -E(I_1 + I_2) \frac{\pi^4}{L^4} \cos(\pi x/L)$, while the distributed shear dislocation, evaluated through (2.6), is $\bar{\gamma}(x) = -\frac{H}{h} \frac{\pi}{L} v_{max} \sin(\pi x/L)$.

In Phase *II* the vertical displacement may be evaluated by solving equation (2.16), together with conditions $v_{II}''(\pm L/2, t) = 0$, $v_{II}(0, t) = \bar{v}(0) = v_{max}$ and $v_{II}'(0, t) = 0$, $\forall t$, and may be written as

$$v_{II}(x, t) = \frac{\alpha^2(t) H^2 A^*}{I_{tot}(\pi^2/L^2 + \alpha^2(t))} v_{max} \left[\cos\left(\frac{\pi x}{L}\right) - 1 \right] + v_{max}, \quad (3.15)$$

where $\alpha(t)$ is defined by (3.3)₂. This means that the beam deformed shape is (co)sinusoidal for all the possible values of the adhesive shear modulus, that is $\forall \alpha(t)$. In the limit cases $G(t) \rightarrow 0$ (Layered) and $G(t) \rightarrow \infty$ (Monolithic), the displacement is

$$v_{II;L}(x) = \lim_{\alpha(t) \rightarrow 0} v_{II}(x, t) = v_{max}, \quad (3.16)$$

$$v_{II;M}(x) = \lim_{\alpha(t) \rightarrow +\infty} v_{II}(x, t) = \bar{v}(x) - \frac{I_1 + I_2}{I_{tot}} \left[\cos\left(\frac{\pi x}{L}\right) - 1 \right]. \quad (3.17)$$

From (2.17) and (2.13) with $M_{II}(x, t) = 0$, one obtains the stress in the beams and in the adhesive layer. Considering the symmetry of the problem and since $\int_{-L/2}^{L/2} \tau_{II}(x, t) dx = 0$, $\forall t$, one finally obtains

$$|\sigma_{i;II}(x, t)| = E \left(\frac{(I_1 + I_2)}{H A_i} + \frac{h_i}{2} \right) \frac{\alpha^2(t) H^2 A^*}{I_{tot}(\pi^2/L^2 + \alpha^2(t))} \frac{\pi^2}{L^2} v_{max} \cos\left(\frac{\pi x}{L}\right), \quad (3.18)$$

$$\tau_{II}(x, t) = \frac{G(t) H}{h(\pi^2/L^2 + \alpha^2(t))} \frac{\pi^3}{L^3} v_{max} \sin\left(\frac{\pi x}{L}\right). \quad (3.19)$$

It is evident from (3.3)₂ that $\tau_{II}(x, t)$ remains bounded even when $G(t) \rightarrow \infty$ ($\alpha(t) \rightarrow \infty$). Figure 7 is the counterpart of Figure 5 for the case a (co)sinusoidal mould. By comparing the two figures, notice that for any given value of $G(t)$ the maximum axial stress in the external plies is slightly higher in the (co)sinusoidal bending than in the constant-curvature bending, but a decrease of more than one order of magnitude can be observed in terms of maximum shear stress.

These conclusions agree with the results obtained in [20], while considering the optimal shape for the cold-bending of laminated glass.

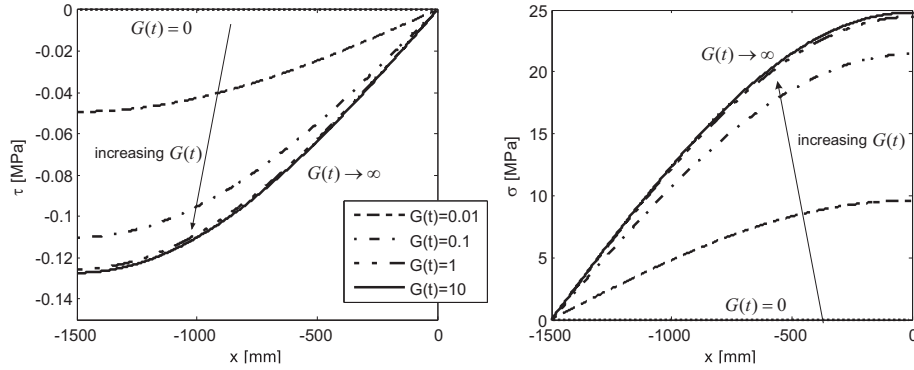


Figure 7: Sinusoidal bent-lamination. Shear stress in the adhesive layer and maximum axial stress in the beams for various values of $G(t)$.

4. Bent-lamination and gradual release

Another way to reduce the stress peaks at the beam ends in phase *II* is to *gradually* release the laminated package from the mould.

Suppose, as in the previous Section, that adhesion process is done when the beam is in perfect contact with the mould, whose curvature K is again supposed to be constant. Phase *I* ends at $t = 0^-$ and Phase *II* begins at $t = 0$. At $t = 0^+$ we suppose that the constraints that maintained the curvature throughout the whole length of the beam have been removed, and that the beam is hold in place by two external forces only, applied at the beam ends as schematically represented in Figure 3a. More precisely, at $t = 0^+$ there is a contact region $d(0^+) = d_I \neq L/2$ under the action of the end forces $P(0^+) = P_I$, and the problem consists in characterizing the type and extension of such contact region, identified by the function $d(t)$, when the end forces $P(t)$ *monotonically* decrease from the initial value $P(0^+) = P_I$ to zero.

Two phases need to be distinguished in the unloading history. In the first one, denoted as “Stage *A*”, the contact zone $d(t)$ gradually diminishes but does not vanish. In this configuration, represented by Figure 8a, the zone $|x| < d(t)$ presents constant curvature K , while the free portions $|x| > d(t)$ are governed by equation (2.14), with a linear bending moment. However, on the contrary to what indicated at beginning of Section 3 (compare Figure 3 and equation (3.2)), the distributed contact reactions $q(x, t)$ in $|x| < d(t)$ are *potentially* non-null. In fact, as it will be shown in Section 4.1, the adhesive layer is now “active” in producing the shear coupling of the laminate.

When $P(t)$ becomes lower than a certain limit value, say P^* , the contact zone reduces to a the point $x = 0$ ($d(t) = 0$), and the contact reaction becomes a concentrated force $2P(t)$, depicted in Figure 8b. This case, referred to as “Stage *B*”, will be investigated in Section 4.2.

To simplify the notation, in the following Sections the subscript *II*, denoting quantities referred to phase *II*, will be omitted without risk of confusion.

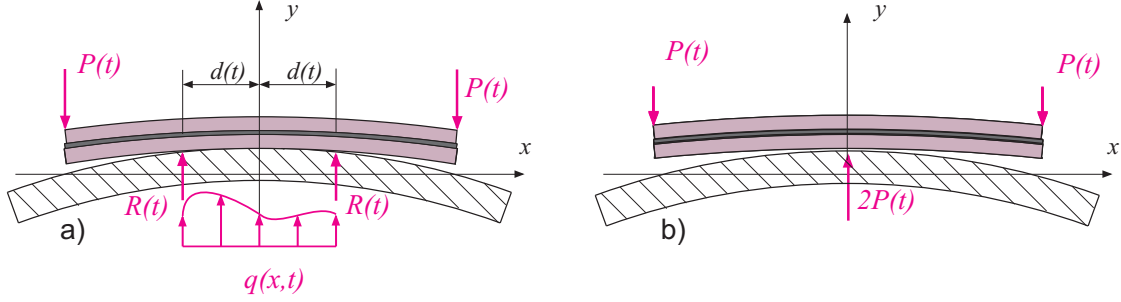


Figure 8: Gradual release of constant-curvature cold-lamination-bending, through decreasing concentrated forces at the beam ends. a) Stage A (distributed contact) and b) Stage B (pointwise contact).

4.1. Stage A: distributed contact

The contact problem is governed by (2.14) with appropriate boundary conditions. With reference to Figure 8a, three different regions need to be distinguished.

- The *central zone* $|x| < d(t)$, here and further denoted by the subscript C , where the beam is in contact with the mould and the vertical displacement is

$$v_C(x) = \frac{K}{2} \left(x^2 - \frac{L^2}{4} \right). \quad (4.1)$$

Since this field is known, (2.14) can be solved to find the bending moment $M_C(x, t)$.

- The two *external zones* $|x| > d(t)$, referred to by the subscript E . Using the symmetry, only the left-hand-side zone $x \in [-L/2, -d(t)]$ needs to be considered. Here the bending moment is $M_E(x, t) = -P(t)[L/2 + x]$ and (2.14) can be used to calculate the vertical displacement.

This is a free-boundary value problem because $d(t)$ is unknown, but it will be evaluated by requiring the continuity of the bending moment⁴ at $x = -d(t)$, that is, $M_E(-d(t), t) = M_C(-d(t), t)$.

4.1.1. Limit cases of null adhesion or stiff adhesion

Consider first the borderline cases of *layered* limit ($G(t) \rightarrow 0$) and *monolithic* limit ($G(t) \rightarrow \infty$), distinguished by the subscripts L and M , respectively.

When $G(t) \rightarrow 0$, the governing equilibrium equation (2.15)₁ may be solved together with boundary conditions (2.9)₁ and (2.9)₂ and continuity conditions for deflection and slope where the central and the external regions meet, i.e., at $x = -d(t)$. In summary, using symmetry, one has

⁴Again, concentrated couples cannot be provided by the constraint reactions because the contact is unilateral.

$$\begin{cases} V_E^*(x, t)|_{x=-L/2} = F, \\ v_E''(x, t)|_{x=-L/2} = 0, \\ v_E(x, t)|_{x=-d(t)} = v_C(x)|_{x=-d(t)}, \\ v_E'(x, t)|_{x=-d(t)} = v_C'(x)|_{x=-d(t)}, \\ M_C'(x, t)|_{x=0} = 0. \end{cases} \quad (4.2)$$

Recalling the definition (2.10) of $V^*(x, t)$, observe that since the adhesive layer is inactive, the first of (4.2) is simply equivalent to $E(I_1 + I_2)v_E''(-L/2, t) = -P(t)$.

With some calculations, one finds the expressions

$$\begin{aligned} M_{C;L}(x) &= EK(I_1 + I_2) = \text{const}, \\ v_{E;L}(x, t) &= -\frac{K}{48} \frac{8x^3 + 12Lx^2 + 24d^2(t)x + 8d^3(t) - 3L^3 + 6L^2d(t)}{L/2 - d(t)}, \end{aligned} \quad (4.3)$$

where the distance $d(t)$ is related to the applied load by the expression, analogous to (3.2),

$$-P(t)[L/2 - d(t)] = E(I_1 + I_2)K, \quad (4.4)$$

which derives from the continuity of the bending moment at $x = -d$.

In the case $G(t) \rightarrow \infty$, the governing equation is given by (2.15)₂, which may be solved simply by prescribing continuity condition on the displacement and slope fields, leading to the following expressions

$$\begin{aligned} M_{C;M}(x) &= EK(I_1 + I_2) = \text{const}, \\ v_{E;L}(x, t) &= -\frac{K}{48} \frac{I_1 + I_2}{I_{tot}} \frac{8x^3 + 12Lx^2 + 24d^2(t)x + 8d^3(t) - 3L^3 + 6L^2d(t)}{L/2 - d(t)} \\ &\quad + \frac{K}{8} \frac{H^2 A^*}{I_{tot}} \left(x^2 - \frac{L^2}{4} \right), \end{aligned} \quad (4.5)$$

where, again, the distance $d(t)$ is related to the applied load by relation (4.4).

Observe that the bending moment in the central region is constant and takes the same value of the layered limit. This is due to the fact that the shear stress field presents jump discontinuities at the frontier points $x = \pm d(t)$, that “shield” the central zone, so that here the state of stress is not affected by the deformation of the external regions.

Both in the monolithic and layered limits, since the bending moment is constant for $x \in [-d(t), d(t)]$, the distributed contact reaction $q_C(x) = -M_C''(x) = 0$ is null. Therefore, the mould reacts with concentrated forces $P(t)$ at $x = \pm d(t)$, which balance the end forces.

4.1.2. Compliant adhesive layer

When the elastic shear modulus of the adhesive layer is finite and nonzero, the displacement field in the central region is known, and the solution of the equilibrium equation (2.14)

in terms of the bending moment $M_C(x, t)$ gives the expression

$$M_C(x, t) = C_{M1}e^{\beta(t)x} + C_{M2}e^{-\beta(t)x} + EK(I_1 + I_2), \quad \beta(t) = \sqrt{\frac{bG(t)}{hEA^*}}, \quad (4.6)$$

whereas in the external regions, where the bending moment is known, the vertical displacement reads

$$v_E(x, t) = \frac{C_1e^{\alpha(t)x} + C_2e^{-\alpha(t)x}}{\alpha^2(t)} + \frac{KH^2A^*x^2}{2I_{tot}} - \frac{P(t)}{2EI_{tot}} \left(\frac{Lx^2}{2} + \frac{x^3}{3} \right) + C_3x + C_4, \quad (4.7)$$

being $\alpha(t)$ as defined in (3.3)₂.

The six constants of integration appearing in such expressions must satisfy the five conditions (4.2), but another condition is necessary for their determination. However, recalling the definition (2.10) for V^* , observe that, in order to satisfy the first of (4.2), it is necessary to know the shear stress $\tau_E(x, t)$. The first derivative of the shear stress field may be evaluated by means of Newmark's equation (2.13), leading to

$$\tau'_C(x, t) = \frac{Gb}{EKHA^*} [C_{M1}e^{\beta(t)x} + C_{M2}e^{-\beta(t)x}], \quad (4.8)$$

$$\tau'_E(x, t) = \frac{E(I_1 + I_2)\alpha^2(t)}{H} [C_1e^{\alpha(t)x} + C_2e^{-\alpha(t)x}]; \quad (4.9)$$

where $\beta(t)$ is defined by (4.6). Hence, the shear stress field in each beam region is determined up to an additive constant.

Therefore, three additional boundary conditions are needed, but some comments are requested. First of all, observe that the shear stress is related with the displacement fields by (2.6) but, since the first derivative of the vertical displacement is continuous, a discontinuity in the shear stress must be associated with a jump in the horizontal displacement fields $u_1(x, t)$ and $u_2(x, t)$, which is not compatible with the kinematic restrictions of the problem. Furthermore, the axial forces acting on the external beams $N_1(x, t) = -N_2(x, t)$ are related to $\tau(x, t)$ by the second and third of (2.11). Hence, a jump discontinuity in the axial forces would result in Dirac delta distribution for the shear stress field that, again, is not compatible with the problem. In conclusion, both the continuity of the shear stress and of the axial forces, resulting in the continuity of the second derivative of the vertical displacement because of (2.12), are required.

In conclusion, the three additional conditions are obtained by requiring that the shear stress is antisymmetric, together with the continuity of the shear stress and of the second derivative of the displacement at $x = -d(t)$, that is

$$\begin{cases} \tau_C(x, t)|_{x=0} = 0, \\ \tau_E(x, t)|_{x=-d(t)} = \tau_C(x, t)|_{x=-d(t)}, \\ v_E''(x, t)|_{x=-d(t)} = v_C''(x)|_{x=-d(t)}. \end{cases} \quad (4.10)$$

The explicit expression for the constant of integrations, as well as the analytic relationship between the applied external actions $P(t)$ and the width of the contact region $d(t)$, can thus be easily determined, but are not recorded here for the sake of brevity. In any case, it should be noted that, for the case of null and of infinite shear modulus of the adhesive layer, $d(t)$ tends to the value predicted by (4.4) whereas the coefficients C_{M1} and C_{M2} of (4.6) tends to zero. Consequently

$$\lim_{G(t) \rightarrow \infty} M_C(x, t) = \lim_{G(t) \rightarrow 0} M_C(x, t) = EK(I_1 + I_2). \quad (4.11)$$

The plots in Figure 9 show the values of $C_{M1} = C_{M2}$ and of the contact radius $d(t)$, as a function of the shear modulus of the adhesive layer $G(t)$, for the same geometry considered in the previous Sections, when the external forces are $P(t) = 3$ kN.

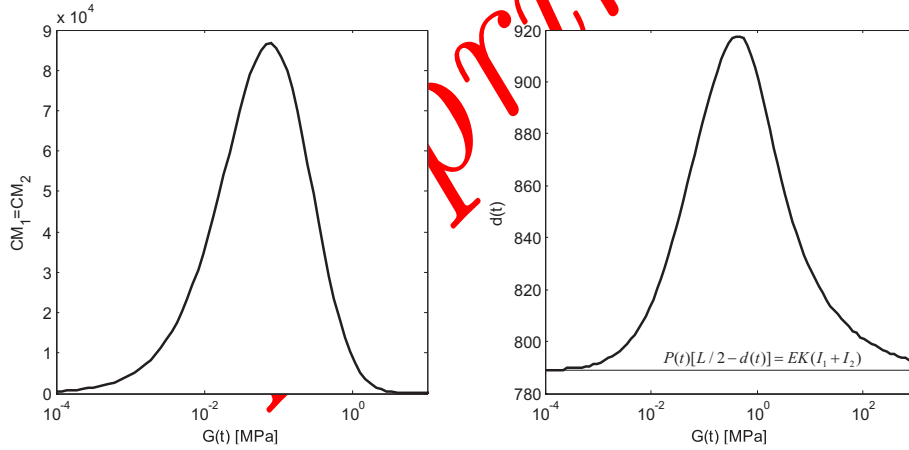


Figure 9: Values of the coefficients $C_{M1} = C_{M2}$ and of the contact radius $d(t)$ as functions of the shear modulus of the adhesive layer. Case $P(t) = 3$ kN.

4.1.3. Results and comparisons.

For the same geometry of the previous section and $P(t) = 3$ kN, Figure 10 shows the vertical displacement as a function of $x \in [-L/2, 0]$, evaluated through (4.1) and (4.7), for different values of the shear modulus of the adhesive layer $G(t)$. In the same Figure, the limit cases of equations (4.3)₂ and (4.5)₂, respectively, are also plotted for the sake of comparison.

Figure 11 shows the graphs of the bending moment, as well as of the axial force in each one of the constitutive beams, for varying $G(t)$. Remarkably the bending moments at the *layered* and at the *monolithic* limits coincide. For intermediate values of $G(t)$ the trend

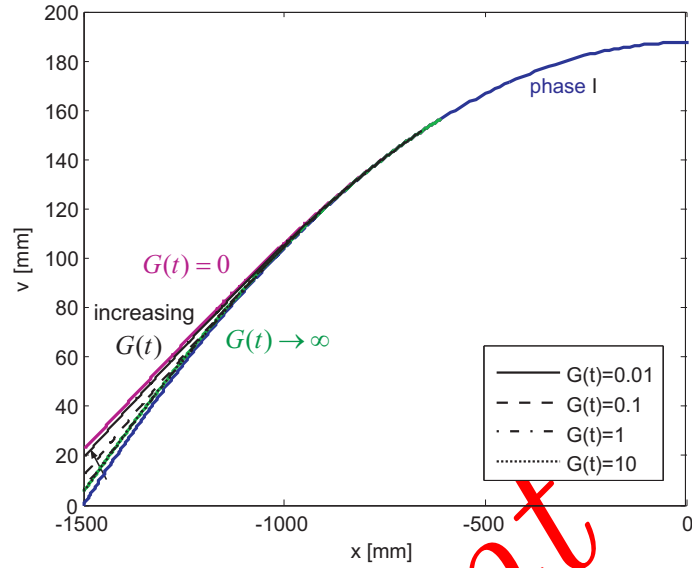


Figure 10: Gradual relaxation, stage A, $P(t) = 3$ kN. Vertical displacement for various values of $G(t)$.

is quite different in the central region, whose radius $d(t)$ obviously depends upon $G(t)$, whereas the external regions are obviously statically determined. On the other hand, the axial force in each constituent beam is null $\forall x$ in the layered limit, while it shows a linear trend in the external region when the monolithic limit is attained. The jump of the axial force at $x = -L/2$ is due to the presence of concentrated shear forces in the adhesive layer at the beam ends, analog to those discussed in Section 3.3 for the case of instantaneous release.

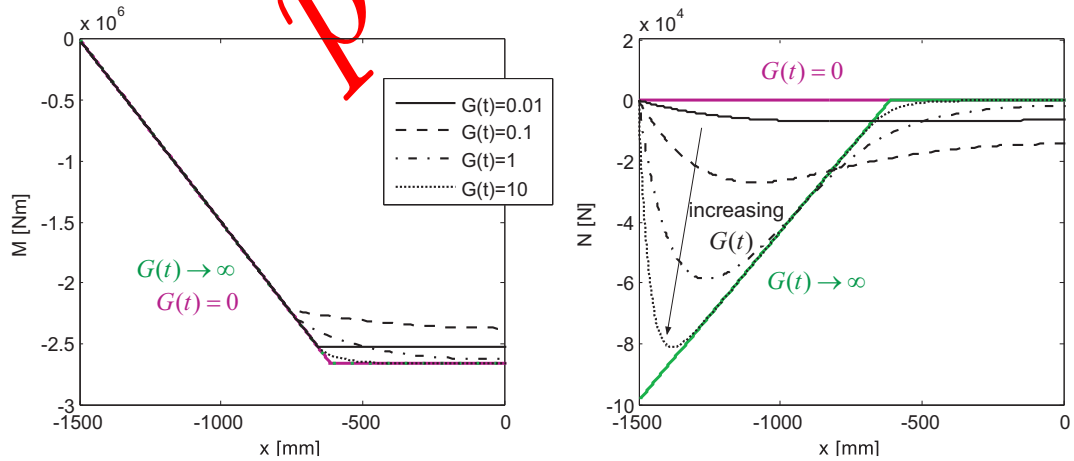


Figure 11: Gradual relaxation, stage A, $P(t) = 3$ kN. Graphs of the bending moment and axial force in each one of the constituent beams for various values of $G(t)$.

The role of the adhesion is even more evident in Figure 12, showing the shear stress

in the interlayer and the absolute value of the maximum longitudinal stress $\sigma_{max}(t)$ in the constituent beams, respectively, as a function of x , for different values of $G(t)$. It should be observed that, as evidenced in Section 4.1.1, in the monolithic limit the shear stress tends to become singular at $x = -L/2$ and exhibits a jump discontinuity at $x = -d(t)$. As a consequence of this, the maximum longitudinal stress is linear.

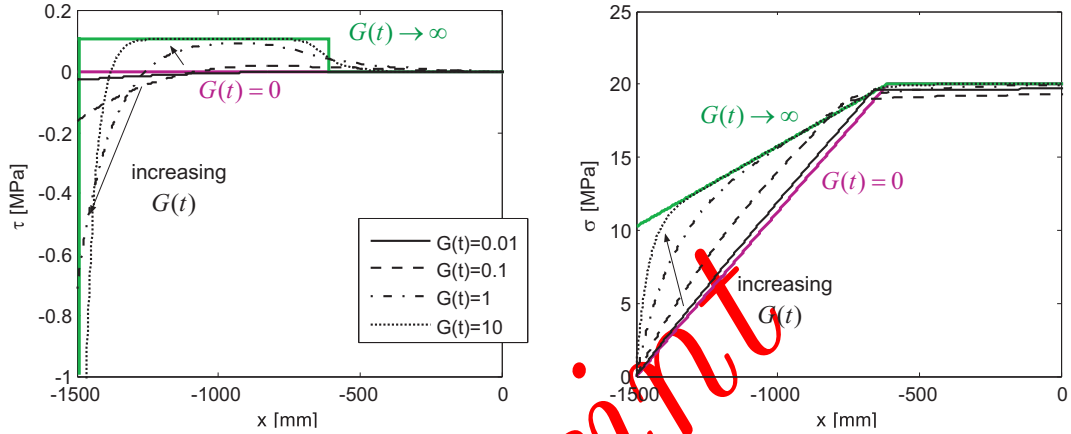


Figure 12: Gradual relaxation, stage A, $P(t) = 3$ kN. Shear stress in the interlayer and axial stress in the constituent beams for various values of $G(t)$.

Figure 13 shows the *distributed* contact reaction between the beam and the mould, that is, the graph $q(x, t) = -M''(x, t)$ in the central region, for different values of the shear modulus of the adhesive layer. Notice that for $G(t) = 0$ one finds $q(x, t) = 0$ because only concentrated forces occur in this case.

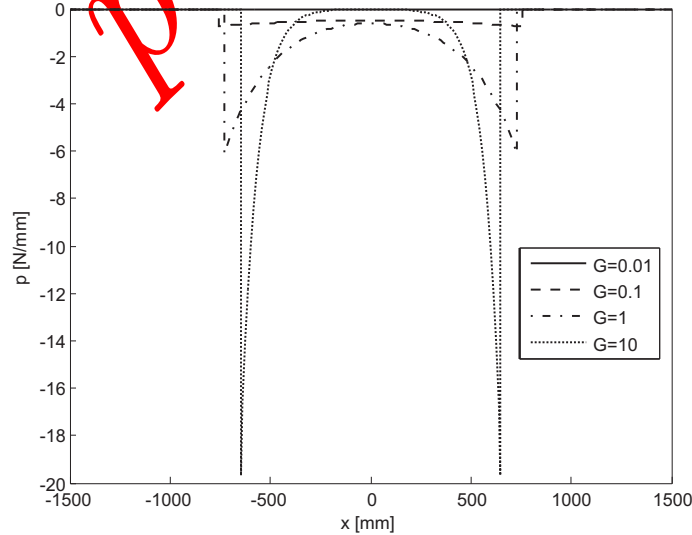


Figure 13: Gradual relaxation, stage A, $P(t) = 3$ kN. Distributed contact reactions with the mould for various values of $G(t)$.

Increasing $G(t)$ the contact reactions are distributed, but they tend to grow unboundedly at $x = \pm d(t)$ when $G(t) \rightarrow \infty$, attaining in the limit the Dirac's distribution because

$$\lim_{G(t) \rightarrow \infty} \int_{-d(t)}^0 q(x, t) dx = P(t). \quad (4.12)$$

On the other hand, in the intermediate cases when $0 < G(t) < \infty$, one can verify that

$$0 < \int_{-d(t)}^0 q(x, t) dx < P(t) \quad \forall t. \quad (4.13)$$

This means that, aside the distributed forces, the mould will exert also concentrated upward reactions at $x = \pm d(t)$ in order to equilibrate the external applied loads.

4.2. Stage B: pointwise contact

There is a value $P(t) = P^*$ for which $d(t) = 0$. Remarkably, since $d(t)$ depends upon the inner layer stiffness properties (see Figure 9b), also P^* depends upon such properties.

4.2.1. Compliant adhesive layer

Consider by symmetry the left-hand-side half beam $x \in [-L/2, 0]$. Differently from stage A, in stage B the bending moment can be determined from statics and read $M(x, t) = P(t)(L/2 + x)$, independently of the value of $G(t)$. Moreover, the contact reaction is a concentrated force $2P(t)$ acting at $x = 0$, as already represented in Figure 8b.

The vertical displacement can be evaluated from (2.14) and reads

$$v(x, t) = \frac{C_1 e^{\alpha(t)x} + C_2 e^{-\alpha(t)x}}{\alpha^2(t)} + \frac{KH^2 A^* x^2}{2I_{tot}} - \frac{P(t)}{2EI_{tot}} \left(\frac{Lx^2}{2} + \frac{x^3}{3} \right) + C_3 x + C_4. \quad (4.14)$$

This expression is the counterpart of (4.7), and the constants can be determined from conditions

$$\begin{cases} V^*(x, t)|_{x=-L/2} = F, \\ v''(x, t)|_{x=-L/2} = 0, \\ v(x, t)|_{x=0} = \bar{v}(x)|_{x=0} = -\frac{KL^2}{8}, \\ v'(x, t)|_{x=0} = 0. \end{cases} \quad (4.15)$$

Again, for the first of (4.15) it is necessary to evaluate the shear stress $\tau(x, t)$ by integrating Newmark's equation (2.13). An additional boundary condition comes from requiring that the distribution of shear stress is antisymmetric, i.e., $\tau(x, t)|_{x=0} = 0$. The explicit expressions for the constant of integration can thus be easily found.

4.2.2. Results and comparisons.

Figure 14 shows the vertical displacement as a function of $x \in [-L/2, 0]$, as *per* (4.14), for different values of the shear modulus $G(t)$, for the same geometry as before and for $P(t) = 0.3 \text{ kN} < P^*$.

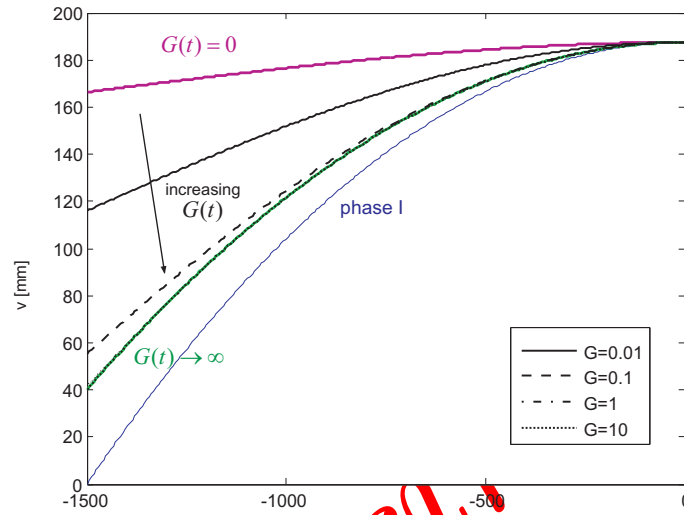


Figure 14: Gradual relaxation, stage B : vertical displacement for various values of $G(t)$.

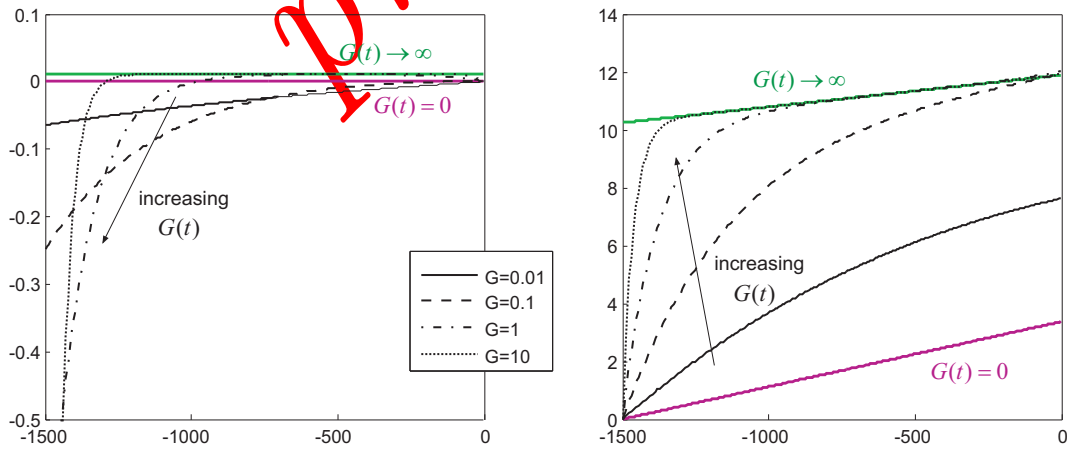


Figure 15: Gradual relaxation, stage B : shear stress in the interlayer and maximum axial stress in the glass plies for various values of $G(t)$.

Figure 15 shows the shear stress in the adhesive layer and the (absolute) value of the maximum longitudinal stress in the external beams as a function of x , for different values of $G(t)$. It is evident that, also in the present case, whenever the monolithic limit is attained ($G(t) \rightarrow \infty$) the shear stress tend to become singular at $x = -L/2$. Comparing this case with that of figure 12, it is evident that the opposite singularities at $x = \pm d(t)$ have merged when $d(t) \rightarrow 0$. The maximum longitudinal stress is obviously linear in the borderline cases of layered and monolithic limits, whereas it is more complicated in the intermediate cases.

4.3. Comparison between instantaneous and gradual release in case of viscoelastic adhesion

This last Section is devoted to the comparisons of the results between the cases of gradual release from the mould (Sections 4.1 and 4.2) and instantaneous release (Section 3). It is evident that the stress state depends not only upon the constraining loads $P(t)$, but also upon the secant shear modulus of adhesive layer, which can vary in time due to viscosity. To illustrate, Figure 16 shows the graphs of the shear stress in the interlayer in $x \in [-L/2, 0]$, for different value of the prescribed external action $P(t)$ (including both stage A and stage B) and of $G(t)$. It is thus evident that there is an interaction between the unloading velocity and the effects of viscosity, which imply that $G(t)$ is a decreasing function of time.

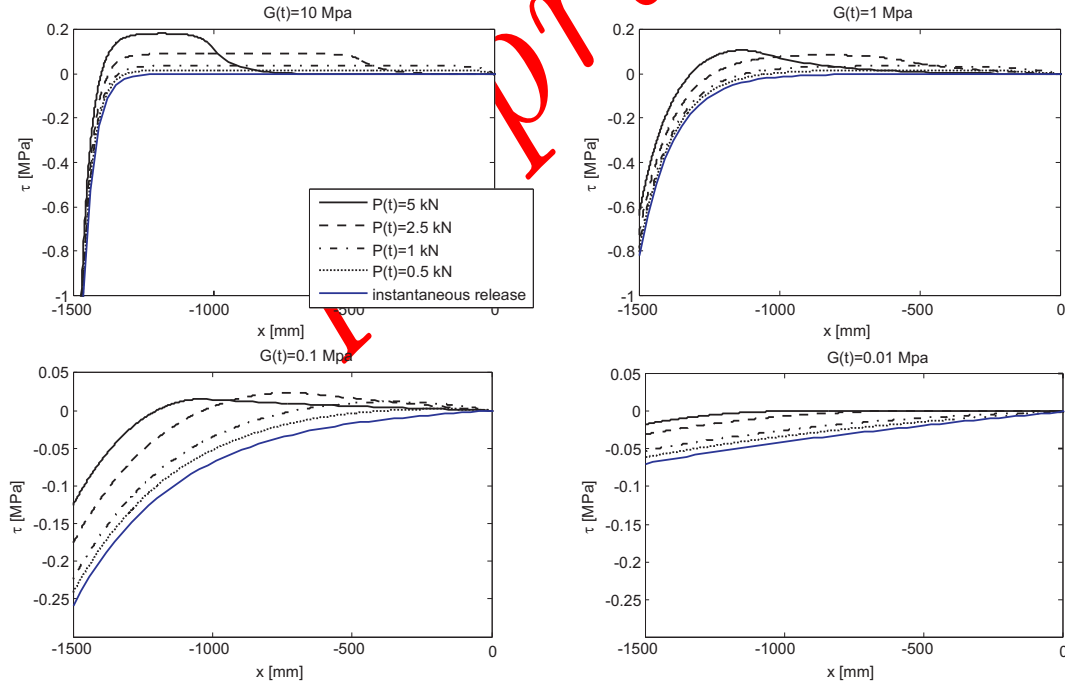


Figure 16: Shear stress transmitted by the adhesive layer, for different value of the prescribed external action $P(t)$ and of the shear stiffness of the adhesive layer (graphs not in the same scale).

Let us consider the case in which the external constraining actions $P(t)$ are linear decreasing function of time, varying from P_I to the null value. For the same geometry of the

laminated package referred to in the previous Sections, suppose that the adhesive layer is made of a viscoelastic material whose response is interpreted through the Maxwell-Wiechert model [18]. More precisely, suppose that under constant shear-strain, the shear modulus decays with time according to the Prony series

$$G(t) = G_\infty + \sum_{k=1}^N G_k e^{-t/\theta_k} = G_0 - \sum_{k=1}^N G_k (1 - e^{-t/\theta_k}), \quad (4.16)$$

where G_∞ is the long-term shear modulus (corresponding to the totally relaxed material), whereas the terms G_k and θ_k , $k = 1, \dots, N$, are respectively the relaxation shear moduli and the relaxation times associated with the i -th Maxwell element. The instantaneous shear modulus G_0 is thus given by $G_\infty + \sum_{k=1}^N G_k$. Assumed parameters for the present case are $N = 3$, $G_0 = 10$ MPa, $G_1 = 9$ MPa, $G_2 = 0.9$ MPa, $G_3 = 0.09$ MPa; $\theta_1 = 1$ s, $\theta_2 = 10$ s, $\theta_3 = 100$ s. Such values are compatible with those of a common glue used to produce glued laminated timber.

Consider, then, the three different unloading histories plotted in Figure 17a, where the descent of the external constraining actions from P_I to the null value is done in 30 s, 60s and 120s, respectively. The value $P_I = 66.7$ kN has been chosen so that the starting detachment-length $d(0^+)$ is of the same order of the beam height.

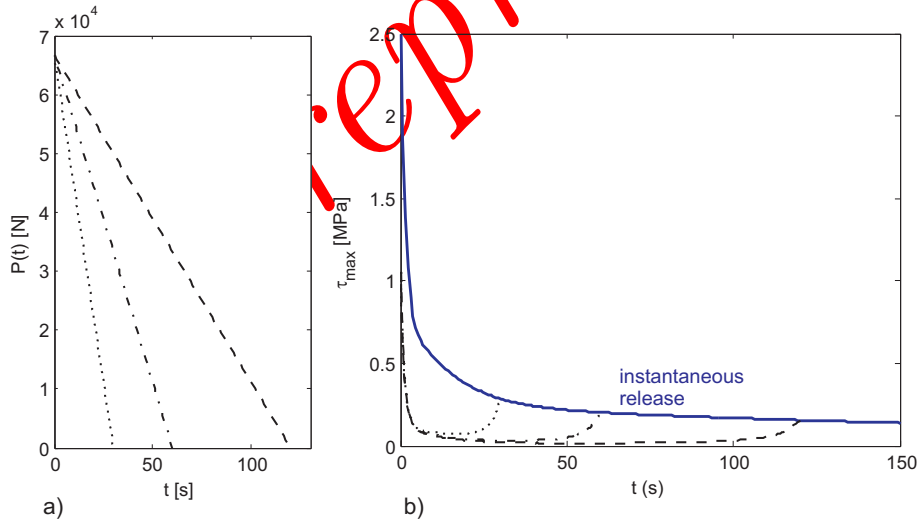


Figure 17: a) Three linear unloading histories. b) Corresponding time-dependent maximum shear stress in the adhesive layer, compared with the shear stress for an instantaneous release.

Figure 17b shows the comparison of the maximum shear stress in the interlayer, obtained in general at the ends $x = \pm L/2$ (Figure 16), for the three considered unloading histories. For the sake of comparison, the graph of instantaneous release, treated in Section 3, is juxtaposed to the others.

Observe that at the instant t in which $P(t) = 0$, the graphs meet, and afterwards follow,

the “instantaneous release” curve. Remarkably, if the constraining loads are gradually removed, the state of stress in the interlayer can be substantially reduced, of one order of magnitude. In other words, a *gradual* release is the way to “bypass” the shear stress concentrations that would occur at the beam ends if the unloading was instantaneous. This case confirms that an accurate design of bent-lamination should not neglect to consider the unloading phase as a crucial part of the process.

5. Conclusions

A model problem has been proposed to describe the response of curved laminated beams obtained by gluing elastic plies while bent against a constraining mould. The composite is made by two Euler-Bernoulli beams bonded, in the deformed state, by a thin viscoelastic adhesive layer, which provides the shear coupling that is necessary to maintain the curvature when the constraints with the mould are removed. However, after the release, the viscoelasticity of the adhesive interlayer provokes an initial spring-back followed by a long-term relaxation due to the decay of the shear-coupling of the constituent plies. This causes not only a time-dependent variation of the shape, but also a redistribution of stress.

The equilibrium equations, as well as the boundary conditions, have been obtained with a variational approach. The relative slip between the beams produced in the forcing phase is properly taken into account as a distributed shear dislocation [7]. The viscoelasticity of the adhesive layer has been considered by assuming that a Prony series for the Maxwell-Wiechert model describes the time-dependence of the shear modulus, an approximation that neglects the memory effect of viscoelasticity [10] and is usually referred to as the *quasi-elastic* approach. The Euler-Lagrange equations may be manipulated by developing, for this particular case, a method originally proposed by Newmark *et al.* [15] for composite beams with elastic interaction, obtaining a fourth-order differential equation for the vertical displacement only. It is then possible to evaluate analytically the relationship between the shape of the mould and the shape of the beam that can be obtained after the release, as well as the resulting state of stress in the constituent layers, which varies with time due to the viscoelasticity of the adhesive.

If the contact is instantaneously released, it is demonstrated that the use of a constant-curvature mould induces remarkable shear stress concentrations in the adhesive layer, in the neighborhood of the beam ends, which can possibly induce delamination. On the other hand, if one applies other types of mould shapes such as the sinusoidal one, which differs only slightly from the constant-curvature configuration in cases of practical importance, an almost uniform distribution of shear stresses can be obtained. Indeed, for what the state of stress is concerned, the constant curvature mould appears to be one of the worst choices, because just a very slight modification of this profile can smoothen out the stress peaks with insignificant modification of the aesthetics.

The possible advantages of a gradual release of the beam have been investigated by solving the time-dependent contact problem of the composite beam with the mould. In particular, the beam is supposed to be pressed against the mould by two time-decreasing external forces applied at its extremities. It has been demonstrated that the viscoelastic

properties of the interlayer strongly influence not only the progressive decrease of the contact area and the redistribution of stress in the constituent layers, but also the qualitative form of the constraint contact reactions. In the limit cases of free-sliding beams (layered limit) or rigidly bonded beams (monolithic limit) the constant-curvature mould exerts concentrated reaction forces at the borders of the contact zone [22]. But when the shear stiffness of the interlayer is non-zero and finite, part of the action of the concentrated contact forces is shifted to a distributed pressure that arises in the contact area.

It is very interesting, in our opinion, to observe that a gradual release from the constraining mould produces a much lower shear stress in the adhesive interlayer with respect to the case of instantaneous release. In other words, a gradual release is the way to bypass the stress concentrations that may occur at the beam ends when the release is instantaneous.

We expect that the present study can furnish indications to optimize the glued laminated timber (Glulam) manufacturing process and the cold-lamination-bending of structural glass. Optimization of the shape of the mould and a proper design of the release phase appear to be crucial factors that can substantially improve the quality of the product, reducing the risks of spontaneous delamination.

Acknowledgements. Support of the European Community European Community under grant RFCS-RFSR-CT-2012-00026 “S+G” is gratefully acknowledged.

- [1] American Society Testing of Materials. D3737. Standard Method for Establishing Stresses for Structural Glued-laminated Timber (Glulam). Pennsylvania: ASTM West Conshohocken; 1992.
- [2] Moody RC, Hernandez R. Glued-laminated timber. In: Smulski S, editor. Engineered wood products - A guide for specifiers, designers and users. Madison, WI: PFS Research Foundation; 1997.
- [3] Behr RA, Minor JE, Norville HS. Structural behavior of architectural laminated glass. *J Struct Eng* 1993;119:202–22.
- [4] Galuppi L, Royer-Carfagni G. Effective thickness of laminated glass beams. New expression via a variational approach. *Eng Struct* 2012;38:53–67.
- [5] Belis J, Inghelbrecht B, Van Impe R, Callewaert D. Cold bending of laminated glass panels. *Heron* 2007;52:123–46.
- [6] Fildhuth T, Knippers J, Bindji-Odzili F, Baldassini N, Pennetier S. Recovery behaviour of laminated cold bent glass-numerical analysis and testing. In: Proceedings of the Challenging Glass 4 and Cost Action TU0905 Final Conference. Lausanne, CH; 2014, p. 113–21.
- [7] Galuppi L, Royer-Carfagni G. Rheology of cold-lamination-bending for curved glazing. *Eng Struct* 2014;61:140–52.

- [8] Williams ML, Landel RF, Ferry JD. The temperature dependence of relaxation mechanisms in amorphous polymers and other glass-forming liquids. *J Amer Chem Soc* 1955;77:3701–7.
- [9] Barredo J, Soriano M, Gómez MS, Hermanns L. Viscoelastic vibration damping identification methods. Application to laminated glass. *Procedia Eng* 2011;10:3208–13.
- [10] Galuppi L, Royer-Carfagni G. Composite beams with viscoelastic interlayer. An application to laminated glass. *Int J Sol Struct* 2012;49:2637–45.
- [11] Galuppi L, Royer-Carfagni G. Buckling of three-layered composite beams with viscoelastic interaction. *Comp Struct* 2014;107:512–21.
- [12] Bardella L, Tonelli D. Explicit analytic solutions for the accurate evaluation of the shear stresses in sandwich beams. *J Eng Mech* 2012;138:502–7.
- [13] Foraboschi P. Three-layered plate: Elasticity solution. *Compos Part B - Eng* 2014;60:764–76.
- [14] Fraternali F, Reddy J. A penalty model for the analysis of laminated composite shells. *Int J Sol Struct* 1993;30:3337–55.
- [15] Newmark NM, Siess CP, Viest IM. Tests and analysis of composite beams with incomplete interaction. *Proc Soc Exp Stress Anal* 1951;9:75–92.
- [16] Puppo AH, Evensen HA. Interlaminar shear in laminated composites under generalized plane stress. *J Compos Mater* 1970;4:204–20.
- [17] Pipes RB, Pagano NJ. Interlaminar stress in laminated composites under uniform axial extension. *J Compos Mater* 1970;4:538–48.
- [18] Wiechert E. Gesetze der elastischen nachwirkung für constante temperatur. *Ann der Phys* 1893;286:546–70.
- [19] Fildhuth T, Knippers J. Dehnungsmessung in gekrümmten glaslaminaten mit faseroptischen sensoren. *Glasbau* 2014;1:289–300.
- [20] Galuppi L, Royer-Carfagni G. Optimal cold bending of laminated glass. Under review 2014;.
- [21] Galuppi L, Royer-Carfagni G. The design of laminated glass under time-dependent loading. *Int J Mech Sci* 2013;49:2637–45.
- [22] Grigolyuk E, Tolkachev V. *Contact Problems in the Theory of Plates and Shells*. Moscow: Mir Pub; 1987.
- [23] Salamon NJ. Interlaminar stresses in a layered composite laminate in bending. *Fibre Sci Technol* 1978;11:305–17.

- [24] Herakovich CT. On thermal edge effects in composite laminates. *Int J Mech Sci* 1976;18:129–34.
- [25] Reedy EDJ. On free-edge interlaminar stress distributions. *Compos Sci Technol* 1989;34:259–66.
- [26] Wu CML. Nonlinear thermal and mechanical analysis of edge effects in angle-ply laminates. *Comput Struct* 1990;35:705–17.
- [27] Nguyen VT, Caron JF. Finite element analysis of free-edge stresses in composite laminates under mechanical and thermal loading. *Compos Sci Technol* 2009;69:40–9.
- [28] Nosier A, Maleki M. Free-edge stresses in general composite laminates. *Int J Mech Sci* 2008;50:1435–47.
- [29] Yazdani Sarvestani H, Yazdani Sarvestani M. Interlaminar stress analysis of general composite laminates. *Int J Mech Sci* 2011;53:958–67.
- [30] Mousanezhad Viyand D, Yazdani Sarvestani H, Nosier A. Stress analysis in symmetric composite laminates subjected to shearing loads. *Int J Mech Sci* 2013;75:16–25.
- [31] Kim RY, Soni SR. Experimental and analytical studies on the onset of delamination in laminated composites. *J Compos Mater* 1984;18:70–80.
- [32] Mortell D, Tanner D, McCarthy C. In-situ SEM study of transverse cracking and delamination in laminated composite materials. *Compos Sci Technol* 2014;105:118–26.